A Novel and Effective Surface Design: Conducting Polymer/β-Cyclodextrin Host−Guest System for Cholesterol Biosensor

Saniye Soylemez,[†] Serife O. Hacioglu,[†] Melis Kesik,[†] Hande Unay,[‡] Ali Cirpan,[†,‡,∇] and Levent Toppare*[,†,‡,§,∇]

[†]Department of Chemistry, Middle East Technical University, Ankara 06800, Turkey
[‡]Department of Polymer Science and Technology, Middle East Technical University, Ankara 06800, Turkey
[§]Department of Biotechnology, Middle East Technical University, Ankara 06800, Turkey
[∇]The Center for Solar Energy Research and Application (GUNAM), Middle East Technical University, Ankara 06800, Turkey

ABSTRACT: The combination of supramolecules and conducting polymers (CPs) has gained much attention for the development of new immobilization matrices for biomolecules. Herein, an amperometric biosensor based on a novel conducting polymer, poly(2-(2-octyldodecyl)-4,7-di-(selenoph-2-yl)-2H-benzo[d][1,2,3]triazole)) (PSBTz) and β-cyclodextrin (β-CD) for the detection of cholesterol, was constructed. The PSBTz film with β-CD was deposited on a graphite electrode by electropolymerization technique to achieve a suitable matrix for enzyme immobilization. Moreover, to justify the immobilization, alkyl chain containing conducting polymer (PSBTz) was designed, synthesized and electrochemically polymerized on the transducer surface. Alkyl chains in the structure of SBTz and hydroxyl groups of β-CD contributed to effective immobilization while protecting the suitable orientation of the biomolecule. Cholesterol oxidase (ChOx) was covalently immobilized onto the modified surface using N,N'-carbonyldiimidazole (CDI) as the cross-linking agent. After successful immobilization, amperometric biosensor responses were recorded at −0.7 V vs Ag/AgCl in phosphate buffer (pH 7.0). The apparent Michaelis-Menten constant (K_M^{app}), maximum current (I_{max}), limit of detection (LOD), and sensitivity values were determined: 28.9 μM, 12.1 μA, 0.005 μM, and 5.77 μA/μM cm^2, respectively. The fabricated biosensor was characterized using scanning electron microscopy (SEM) and cyclic voltammetry (CV) techniques. Finally, the prepared biosensor was successfully applied for the determination of cholesterol in blood samples.

KEYWORDS: conducting polymer, β-cyclodextrin, cholesterol biosensor, cholesterol oxidase
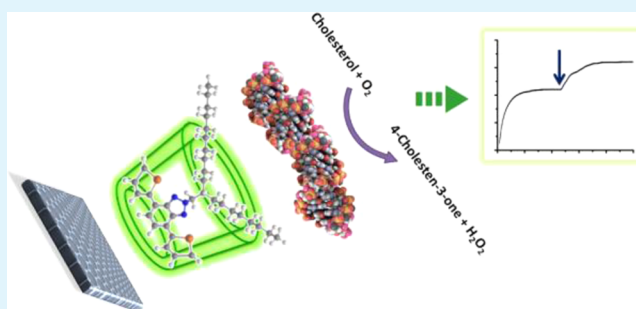
1. INTRODUCTION

Cyclodextrins (CDs) are cyclic oligosaccharides that are composed of α-D-glucopyranoside units linked in 1,4-positions.[1] α-CD (6 units), β-CD (7 units), and γ-CD (8 units) are examples that exhibit the different sizes of the molecular cavities. This particular confirmation leads to a certain selectivity toward host structures. Characteristically, the molecular truncated cone structure of the CDs includes two hydroxyl groups: the smaller rim bears primary hydroxyl groups and the larger rim carries secondary hydroxyl groups.[2] Besides these hydrophilic top and bottom cavities, the cone is composed of six-membered glucopyranoside units containing C−H groups and glycosidic oxygen, which supplies hydrophobic character. Being hydrophobic inside and hydrophilic outside, together with the presence of two types of hydroxyl groups in their molecular structure, enables them to form new supramolecular complexes with a variety of molecules possessing interesting properties. Therefore, CDs have been attracted great interest in several application fields in chemistry. Also, because of their properties, such as biocompatibility and nontoxicity, CDs have found use in the medicine, cosmetics,

and pharmaceuticals industries.[3] In particular, β-CD provides an ideal geometry to create a host−guest system for several molecules, such as biotin,[4] pyrrole,[5] or poly(acrylic acid),[6] etc. Their particular geometry to form supramolecular complexes with desirable properties provides proper biomolecule deposition in biosensing systems.

CPs have noteworthy electrochemical, structural, and optical properties making them applicable in many research fields.[7,8] They exhibit excellent conductivity and high mechanical strength, and their processability leads to the development of new materials in many research areas. Since CPs enable structural and electronic modifications, superior properties of CPs can be generated for the desired purpose. Considering that CPs have the ability to mimic the natural environment for biomolecules, CPs are charming materials for the immobilization of biomolecules in biosensor construction.[9−11] The ingenious concept of combining the biorecognition element

Scheme 1. Preparation of the Proposed Biosensor
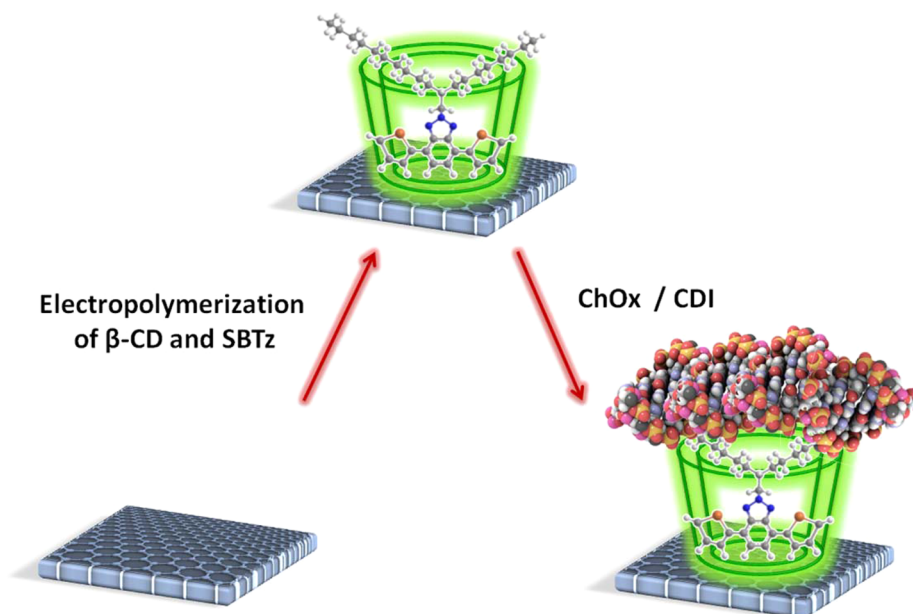
with the sensitivity of transducers has led to the development of biosensors as sensitive and selective tools.[12] Since most of the transducers used for biosensor construction are made of CPs, the biomolecule deposition of electropolymerized films is one of the few methods that have attracted much attention. Electropolymerization is a simple method that leads to the reproducible growth of organic film with easy control of polymer formation on the electrode surface.[13] Furthermore, surface morphology can be adjusted by arranging the thickness of the polymer film. In this way, these types of transducers offer extensive stability for the enzyme. Hence, considering their compelling properties, electropolymerized films are promising materials for biomolecule immobilization in biosensing systems.

Molecular design plays a crucial role in the development of support materials. Unique properties of each molecule can be associated in a new macromolecule that has superior properties than those of the pristine ones. In this way, it is possible to generate several properties in a structure that make it useful for the desired purpose. Associating the macromolecules with CDs can lead to interesting properties.[14−16] The resulting feature reveals fascinating biomaterials that mimic natural proteins; hence, new versatile functions are created through synergic effect of polymeric structures with CDs. There are numerous studies for elaboration of polymeric units onto CDs with different strategies. Ritter et al. reported on water-soluble *N*-methacryloyl-11-aminoundecanoic acid/*β*-CD complex and the polymerization behavior of this pseudo-rotaxane in an aqueous medium.[17] Ovsejevi and co-workers synthesized thiol-*β*-CD to control polyphenol oxidase activity.[18] Adeli et al. synthesized amphiphilic co-polymers containing a CD core with poly(lactide) and poly(oxazoline) arms and investigated loading of the guest molecules by amphiphilic co-polymers.[19] Among all these methods, electropolymerization is one of the easiest methods to achieve newly designed supramolecule host−guest systems. There is no need to arrange several parameters, because it is a one-step preparation. It also does not require further purification processes. Moreover, this method enables co-polymerization of each substructure simultaneously, which allows the formation of the target supramolecular system in a

solid support. Hence, incorporation of conducting polymers onto CDs via electropolymerization opens a new perspective in the field of enzyme immobilization.

Biosensors are widely used in many areas of clinical analysis, such as environmental monitoring and the food industry.[20−22] A biosensor device consists of a sensitive biorecognition element intimately associated with a transducer element that converts the biological response to an electrical signal. The measured signal is a response of the biosensor for a specific analyte in any test solution.[23] Cholesterol monitoring is one of the most studied topics in biosensors since determination of the cholesterol concentration in blood is a considerably important factor for human health. An increase in cholesterol is related to various clinical disorders, such as heart disease, arteriosclerosis,[24] hypertension,[25] and diabetes,[26] whereas a low level of cholesterol is associated with conditions such as anemia, wasting syndrome, etc.[27] Therefore, in the past decades, considerable effort has been devoted to the construction of biosensors for biochemical analyses, because of their high sensitivity, stability, reproducibility, and low cost.[28,29] [The mechanism used to form these biosensors is depicted in Scheme 1.] For this purpose, amperometric cholesterol biosensors have been proposed. ChOx is a model enzyme that catalyzes the oxidation of cholesterol by molecular oxygen to 4-cholesten-3-one and hydrogen peroxide upon applied potential.

The motivation of this study is to describe an alternative approach for the easy preparation of biosensing surface based on a poly(2-(2-octyldodecyl)-4,7-di(selenoph-2-yl)-2*H*-benzo-[*d*][1,2,3]triazole)) (PSBTz)-bearing *β*-CD with the objective of providing an enhanced biosensor performance, as well as improving immobilization platform. Immobilization via supramolecular interactions using *β*-CD as the anchor molecule has the advantage of having modified surfaces that contribute fast and selective determination of the cholesterol. Besides, its suitable immobilization platform properties promote a robust covalent attachment of the biomolecule on the surface. The accuracy and reliability of the biosensor was tested by determining the cholesterol concentration in serum samples.

Scheme 2. Synthesis Pathway of SBTz
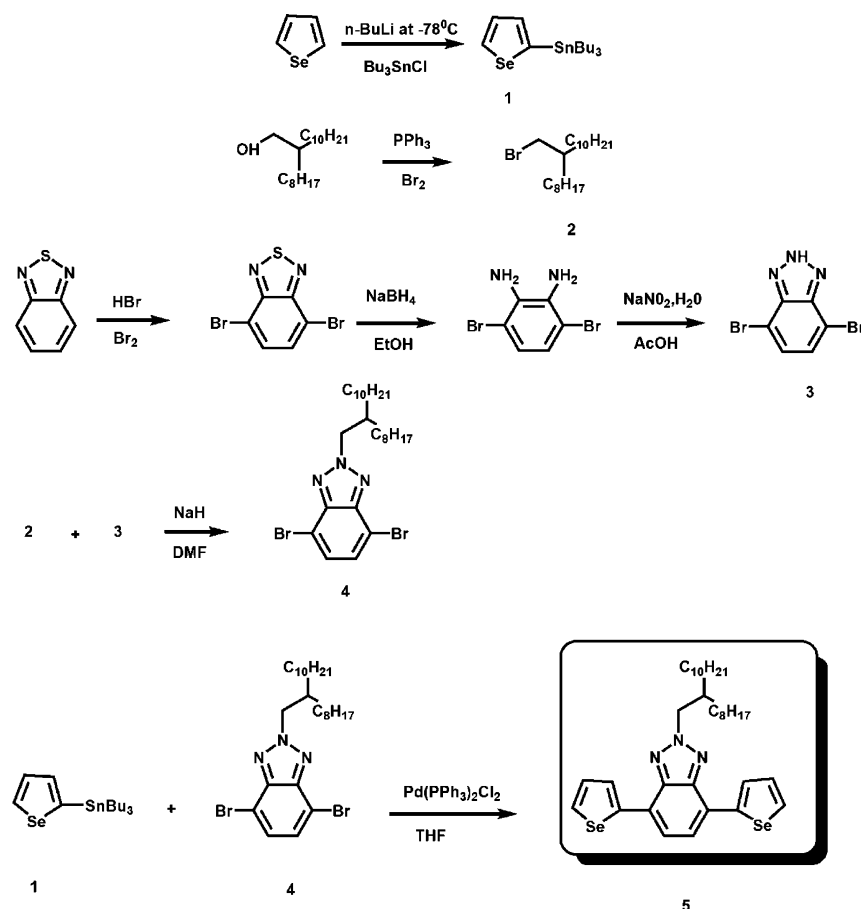
2. EXPERIMENTAL SECTION

ChOx (E.C.1.1.3.6) (37 U/mg protein) from *Streptomyces sp.*, cholesterol, Triton-X 100, CDI, and β-CD were purchased from Sigma–Aldrich and used with no further purification. A solution of cholesterol (0.005 M) was freshly prepared by dissolving cholesterol in 1% (v/v) Triton-X 100 in 2-propanol (Merck). To obtain a clear solution, it was then diluted with 50 mM phosphate buffer solution (PBS) (pH 7.0), consisting of 0.025 M Na_2HPO_4 (Fisher Scientific Company) and 0.025 M NaH_2PO_4 (Fisher Scientific Company), and distilled water. Dichloromethane (DCM) and acetonitrile (ACN) were purchased from Merck (Darmstadt, Germany). Tetrabutylammonium hexafluorophosphate ($TBAPF_6$) was supplied by Aldrich. The chemicals used in the synthesis of the monomer were purchased from Sigma–Aldrich. All other chemicals were analytical grade.

2.1. Apparatus. All amperometric measurements were performed using potentiostat EmStat (PalmSens, Houten, The Netherlands, www.palmsens.com) in a three-electrode cell configuration consisting of a graphite electrode (Ringsdorff Werke GmbH, Bonn, Germany, type RW001, diameter of 3.05 mm and 13% porosity) as the working electrode. A platinum wire was used as the counter electrode. Measurement of amperometric analyses were calculated as the average of four measurements and standard deviations were given as ±SD. Scanning electron microscopy (SEM) (JEOL, Model JSM-6400) was used to investigate the surface morphology of the constructed cholesterol biosensor. Cyclic voltammetry studies were performed with a GAMRY Reference 600 potentiostat

(GAMRY Instruments, Inc., Warminster, PA, USA). Spectroelectrochemical studies of the polymer films were performed with Varian Model Cary 5000 UV−vis spectrophotometer. Structures were proven by nuclear magnetic resonance (NMR) spectra recorded on a Bruker Model Spectrospin Avance DPX-400 spectrometer with trimethylsilane (TMS) as the internal reference.

2.2. Synthesis of 2-(2-octyldodecyl)-4,7-di(selenoph-2-yl)-2Hbenzo[d][1,2,3]triazole))(SBTz) (5). Tributyl-(selenophen-2-yl)stannane (**1**), 9-(bromomethyl)nonadecane (**2**), and 4,7-dibromo-2-(2-octyldodecyl)-2H-benzo[*d*][1,2,3]-triazole (**4**) were synthesized according to previously described methods.[30,31] Structures of monomer and intermediates were proven by NMR spectra. 4,7-Dibromo-2-(2-octyldodecyl)-2H-benzo[*d*][1,2,3]triazole (852 mg, 1.53 mmol) and tributyl-(selenophen-2-yl)stannane (2.8 g, 6.67 mmol) were dissolved in tetrahydrofuran (THF) (100 mL). Bis(triphenylphosphine)-palladium(II) dichloride (135 mg, 0.19 mmol) was added into the solution and the reaction mixture was refluxed for 18 h under argon atmosphere. After the reaction was completed, the solvent was removed under reduced pressure. Column chromatography was performed by silica gel using petroleum ether and DCM (10:1) as the eluents, and product was obtained as a yellow solid (790 mg, 78% yield) (see Scheme 2). HRMS: calculated $[M]^+$ = 660.2360, measured $[M]^+$ = 660.2335.

^{1}H NMR (400 MHz, $CDCl_3$), δ (ppm): 8.1 (dd, J1 = 0.95 Hz, J2 = 2.90 Hz, 2H), 7.9 (dd, J1 = 0.95 Hz, J2 = 4.68, 2H) 7.5 (s, 2H), 7.32 (dd, J1 = 1.73 Hz, J2 = 3.89 Hz, 2H) 4.64 (d, J =

18292

dx.doi.org/10.1021/am5054493 | *ACS Appl. Mater. Interfaces* 2014, 6, 18290−18300

6.42 Hz, 2H), 2.18 (m, 2.14−2.23, 1H), 1.25 (m, 1.12−1.32, 32H), 0.78 (m, 0.74−0.82, 6H). ^{13}C NMR (400 MHz, CDCl$_3$), δ (ppm): 143.7, 140.3, 130.0, 128.9, 126.6, 123.9, 121.3, 75.6, 75.3, 37.7, 30.5, 30.4, 30.1, 28.4, 28.2, 28.1, 27.9, 24.9, 21.3, 12.7.

2.3. Biosensor Preparation. PSBTz and β-CD were electrochemically prepared on previously cleaned graphite electrodes. Electropolymerization was carried out in an aqueous solution containing 0.1 M TBAPF$_6$, 3 mM SBTz, and 0.6 mM β-CD in 5:95 (v/v) DCM:ACN solution (total volume of 2 mL) with repeated scan intervals between −0.3 V and 1.5 V via cyclic voltammetry with a scan rate of 100 mV s^{-1} (see Figure 5A, presented later in this work). For this reason, 6 M aqueous stock solution of β-CD was prepared. Three millimolar (3 mM) SBTz solution was prepared in 5:95 DCM:ACN with a 0.1 M TBAPF$_6$ electrolyte. Two microliters (2 μL) of β-CD stock solution was injected into a monomer solution and 20 cycles of CV were run to coat the electrode surface. The modified electrode then was immersed in a 30 M CDI solution (0.06 g of CDI dissolved in 2 mL of distilled water) and left for overnight in a refrigerator for the activation of the hydroxyl groups of β-CD using CDI chemistry. Finally, 2.5 μL (0.3 U) ChOx was spread over the modified surface for the construction of a robust cholesterol biosensor. Here, interactions between a biomolecule and exterior free hydroxyl groups of β-CD should be tough, to achieve efficient enzyme immobilization. Subsequently, these hydroxyl groups of β-CD were activated via CDI. This helps the linkage of amino groups of ChOx with hydroxyl groups.[32] After the enzyme immobilization, electrode surface was left to dry at room temperature for 3 h and stored at +4 °C overnight to obtain amperometric responses.

2.4. Measurement Procedure. Amperometric biosensor measurements were done under ambient conditions in a cell containing 10 mL 50 mM PBS, pH 7.0 under mild stirring. During the amperometric measurements, after the background signal reached a steady state, a certain amount of cholesterol was injected into the reaction cell. Amperometric responses were recorded by detecting the change in current. After each measurement, the electrode was washed with distilled water and the working buffer was refreshed. In amperometric studies, the decrease in oxygen level was determined as the analytical signal at −0.7 V vs Ag/AgCl and correlated with the substrate concentration. During the experiments, a cholesterol solution was prepared freshly and stored in darkness at room temperature.

3. RESULTS AND DISCUSSION

3.1. Electrochemical, Spectroelectrochemical, and Kinetic Properties of SBTz. *3.1.1. Electrochemical Properties.* The SBTz monomer was electrochemically polymerized via CV by sweeping the potential between 0.0 and 1.5 V. After the synthesis of PSBTz in 0.1 M TBAPF$_6$/DCM:ACN, further CV studies were performed to investigate the redox properties in 0.1 M TBAPF$_6$/ACN at a scan rate of 100 mV s^{-1}.

In the first cycle of repeated potential scan electropolymerization, the irreversible monomer oxidation peak was recorded at 1.18 V for SBTz. With consecutive cycles, observation of a new reversible redox couple with an increasing current intensity illustrates the formation of an electroactive polymer film (see Figure 1A).

In addition to redox behaviors, both HOMO−LUMO energy levels and *p*-type/*n*-type doping properties of the resulting polymer PSBTz were also explored using the same solvent
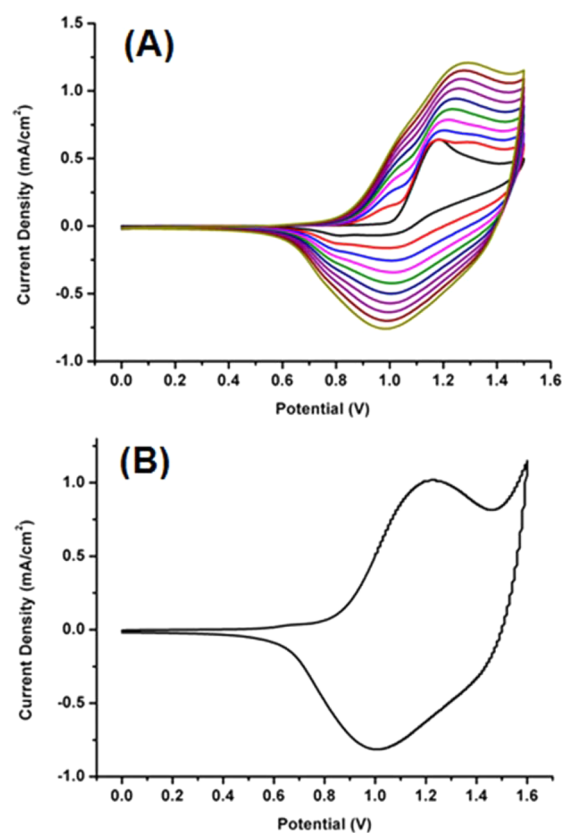

Figure 1. (A) Repeated potential scan electropolymerization of PSBTz at 100 mV/s in 0.1 M TBAPF$_6$/DCM:ACN (5:95, v/v) solution by sweeping the potential between 0.0 and 1.5 V on an ITO electrode (up to 10 cycles). (B) Single scan cyclic voltammogram of PSBTz in a monomer-free 0.1 M TBAPF$_6$/ACN solution.

supporting electrolyte couple, as reported in Figure 1B. PSBTz has *p*-doping property with a reversible redox couple at 1.22 V/1.00 V. The HOMO energy level of the polymer was calculated as −5.88 eV from the onset of the oxidation by calibrating the reference electrode against Fc/Fc+ and calculating the energy levels relative to the vacuum level. As mentioned previously, PSBTz shows only *p*-doping property; hence, LUMO energy level could not be calculated from cyclic voltammograms. Instead, it was determined as −4.06 eV using the optical-band-gap value and the HOMO energy level (Table 1).

In order to probe the scan rate dependence of the anodic/cathodic peak currents, cyclic voltammograms were recorded at different scan rates (50, 100, 150, 200, 250, and 300 mV/s) in a monomer-free medium, and the results are summarized in Figure 2. This linear dependence illustrates the formation of well-adhered polymer films and the nondiffusion controlled doping/dedoping processes.

3.1.2. Spectroelectrochemistry. The change in electronic absorption spectra via stepwise oxidation offers a chance to correlate the optical responses of the polymer films with their structures. In this way, one can get deep perspective on structure−property relations, which enables one to design the synthesis of functional polymers with proper modifications on the polymer backbone. Spectroelectrochemical studies of the PSBTz were carried out using an ultraviolet−visible−near-infrared (UV-Vis-NIR) spectrophotometer in a 0.1 M monomer-free TBAPF$_6$/ACN solution via incrementally increasing the potential between 0.0 V and 1.2 V.

Table 1. Summary of Electrochemical and Spectroelectrochemical Properties of PSBTz

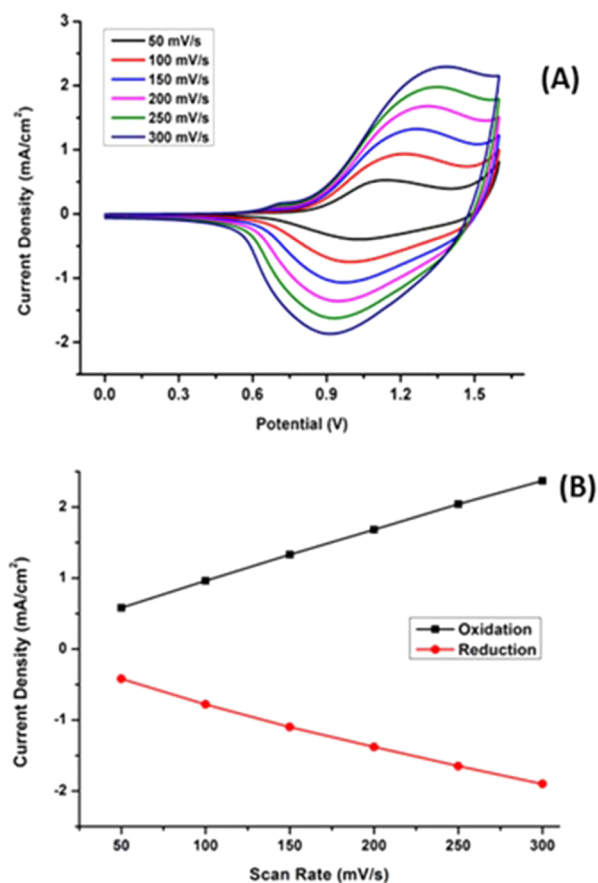|	E_m^{ox}	$E_{p\text{-doping}}$ (V)	$E_{p\text{-dedoping}}$ (V)	HOMO (eV)	LUMO (eV)	λ_{max} (nm)	E_g^{op} (eV)
PSBTz	1.18	1.22	1.00	−5.88	−4.06	527	1.82

Figure 2. (A) Scan rate dependence of PSBTz at 50, 100, 150, 200, 250, and 300 mV/s. (B) Related oxidation/reduction plots.

After applying constant potential to remove any trapped charge and dopant ion coming from electrochemical polymerization, neutral film absorption was recorded. Later, stepwise oxidation was performed. The potential ranges were determined in accordance with the CV results (Figure 3A). As seen in Figure 3A, during stepwise oxidation, as the absor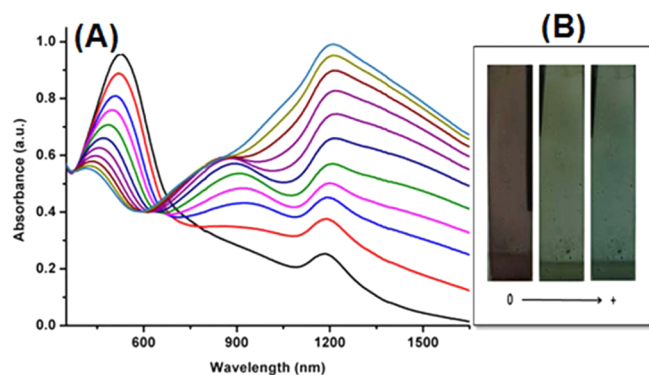ption in the visible region decreased, new absorption bands (namely, polaron and bipolaron bands) appeared (at 860 and 1220 nm, respectively).

PSBTz has a maximum absorption wavelength in the visible region centered at 527 nm. Consistent with its neutral absorption maxima, the corresponding polymer exhibits a purple color in its neutral state, as reported in Figure 3B. The optical band gap of PSBTz was calculated from the onset of the lowest-energy $\pi-\pi^*$ transition to be 1.82 eV. According to the calculated E_g value, PSBTz can be regarded as a low-band-gap polymer, which makes it applicable in different research fields. As illustrated in Figure 3B, in the neutral state, PSBTz has s purple color. Further oxidation results in a blue color in the fully oxidized state, with green color intermediates.

3.1.3. Electrochromic Contrast and Switching Studies. Switching time can be defined as the time required for one full switch between neutral and oxidized states of a polymer. The ability of a polymer to change its color between two extreme states rapidly with significant color change is very important for electrochromic applications.

The switching times of PSBTz and the percent transmittance changes (optical contrasts) at polaron and bipolaron regions were explored via kinetic studies. The kinetic studies were performed in 0.1 M TBAPF$_6$/ACN solution between the neutral and fully oxidized states of the polymer by applying potentials at intervals of 5 s. The corresponding wavelengths were determined from electronic absorption maxima as 860 and 1120 nm.

Potential was swept between the neutral (0.0 V) and oxidized (1.4 V) states to illustrate a percent transmittance of 40% at 1220 nm and 16% at 860 nm (Table 2). The recorded switching times at corresponding wavelengths and mentioned potentials were 1.5 and 4.2 s, respectively (see Figure 4).

Table 2. Summary of Kinetic and Optical Studies of PSBTz

	optical contrast (%)	switching time (s)
1220 nm	40	1.5
860 nm	16	4.2

Figure 3. (A) Electronic absorption spectra for PSBTz in 0.1 M TBAPF$_6$/ACN solution between 0.0 and 1.2 V. (B) Colors of the PSBTz film under different applied potentials.
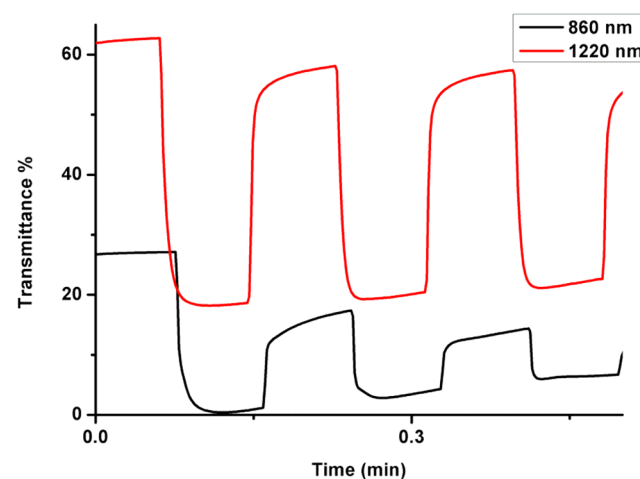

Figure 4. Optical contrasts and switching times monitored at different wavelengths for PSBTz film in 0.1 M TBAPF$_6$/ACN solution.

3.2. Electrochemical Polymerization of the SBTz Containing β-CD.

Figure 5 shows cyclic voltammograms of the combination of PSBTz with β-CD film on the electrode surface. Electropolymerization was performed by mixing certain amounts of β-CD and SBTz in 0.1 M TBAPF$_6$/5:95 DCM:ACN solution with repeated scan intervals between −0.3 V and 1.5 V with a scan rate of 100 mV s^{-1} (Figure 5A). As mentioned above, pristine SBTz was electropolymerized in 0.1 M TBAPF$_6$/5:95 DCM: ACN solution at 0.0 and 1.5 V with a scan rate of 100 mV s^{-1}. In this study, β-CD with a hydrophobic internal cavity and a hydrophilic outer surface and SBTz, which has an alkyl chain on its backbone, were combined as an alternative immobilization matrix to fabricate biosensor to form an effective surface layer. Covalent bonds were used to merge hydroxyl groups of β-CD and amine groups of enzyme molecule. It was reported that after the incorporation of polymer chains into the β-CD, polymer networks can be easily formed due to inclusion interactions.[33,34]
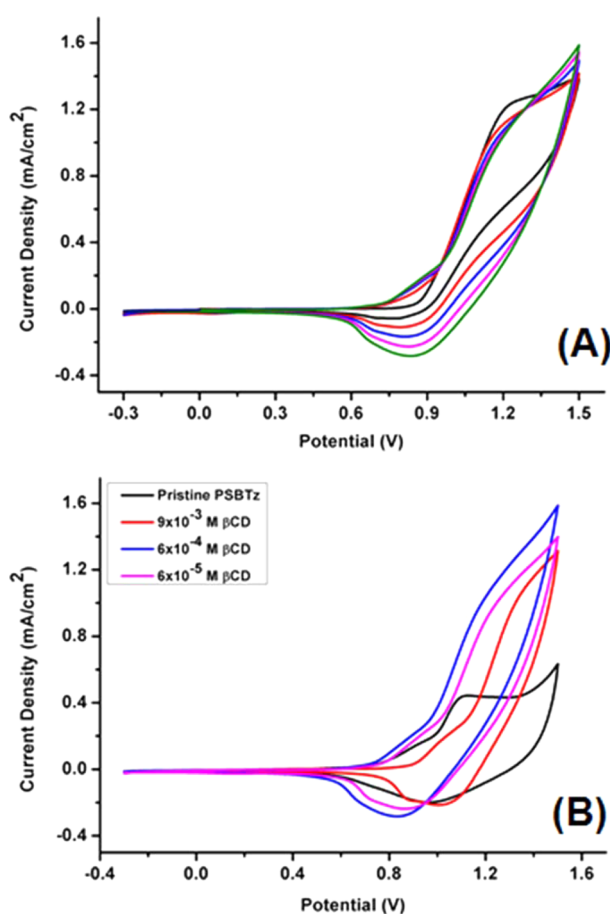

Figure 5. Cyclic voltammograms of (A) PSBTz/β-CD modified electrode from 3 mM SBTz + 0.6 mM (in 2 mL) β-CD + 5:95 DCM:ACN solution containing TBAPF$_6$ (up to 5 cycles) and (B) fifth cycles of PSBTz and PSBTz/β-CD at different β-CD concentrations.

Furthermore, to get the best combination for a high biosensor performance, the β-CD content was tested. Different concentrations of β-CD were prepared (9×10^{-3}, 6×10^{-4}, and 6×10^{-5} M) in the polymerization solution. As shown in Figure 5B, the highest charge involved in the film formation was calculated as 16.02 mC for the optimum electrode (6×10^{-4} M for β-CD/PSBTz). When the β-CD amount was increased or

decreased, charge was calculated as 10.4 mC for 9×10^{-3} M β-CD/PSBTz and 13.88 mC for 6×10^{-5} M β-CD/PSBTz, respectively. For the pristine PSBTz, the charge was calculated to be 9.42 mC. Such differences can prove proper modification of the electrode surface with β-CD. When the concentration of β-CD was increased in the monomer solution, the charge deposition of the films decreased (Figure 5B). This may be associated with the slower electron transfer from the electrode, which is due to the presence of an insulating β-CD composite film.[35] Moreover, the reduction in current may hinder one from obtaining a proper and homogeneous film, because of the excess presence of β-CD on the electrode surface. In addition, diffusion problems may occur because of the limited electron transfer from the enzyme molecule to the polymer's active center. On the other hand, with low amounts of β-CD, the enzyme molecule could not be fixed onto the PSBTz/β-CD-coated surface, which results in leaching of the enzyme from the electrode surface. Hence, maximum interaction and satisfactory immobilization of the enzyme molecules were achieved with an optimum amount of β-CD. Furthermore, differences can be observed the position of the oxidation peaks (Figure 5B). For the pristine PSBTz, the oxidation peak was found at $E_{ox} = 1.12$ V, whereas for the optimum electrode of PSBTz/β-CD, the peak was observed at $E_{ox} = 1.20$ V. The difference was calculated as $\Delta E_{ox} = 0.08$ V. This slight difference proves the modification of the electrode surface. Moreover, independent of the β-CD concentration in the solution, the general trend was observed as a shift to a higher oxidation potential in the presence of β-CD. This is illustrated in Figure 5B.

In addition, the presence of β-CD in the polymer film was proven via UV-vis absorption spectroscopy. To further investigate the β-CD and PSBTz film formation on the electrode surface, absorption spectra of pristine PSBTz and PSBTz/β-CD were recorded. Pristine PSBTz film exhibits a purple color in its neutral state, as shown in Figure 6. Since PSBTz is purple and β-CD is colorless (absorbs in the UV region), increasing the β-CD ratio decreased the absorption intensity in the visible region and shifted the absorption to lower wavelengths. On the other hand, decreasing the β-CD ratio increased the absorption intensity in the UV region and shifted the absorption to higher wavelengths.
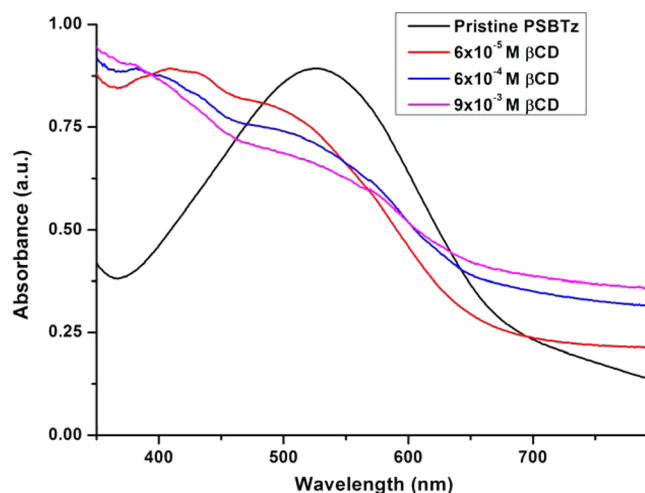

Figure 6. UV-vis absorption spectra for pristine PSBTz and after the insertion of β-CD into the polymer structure at different concentrations.

3.3. Optimization Studies of the Biosensor.

Protection of the activity of the biomolecule on the electrode surface is a key parameter in establishing a biosensor. Successful preparation of the effective surface depends on the surface characteristics, the characteristics of the chosen materials, and the biological properties of the enzyme molecules while protecting their 3D structure.

When pristine PSBTz was coated on the electrode surface, amperometric signals decreased, compared to thae observed with β-CD (see Figure 7A). The presence of pristine
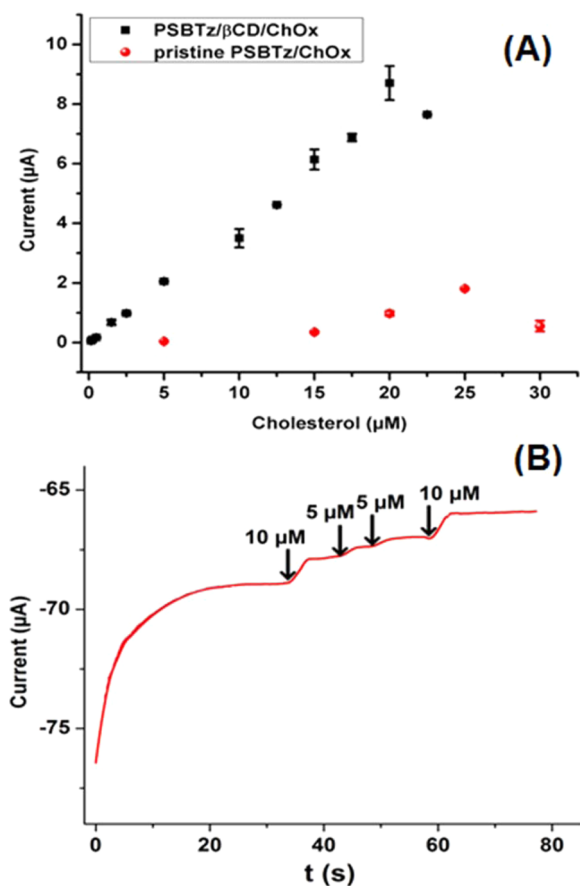
Figure 7. (A) Effect of β-CD on PSBTz/ChOx biosensor (in 50 mM PBS, pH 7.0, 25 °C, −0.7 V); error bars show the standard deviation (SD) of three measurements. (B) Amperometric response of the PSBTz/β-CD/ChOx after successive additions of 10 and 5 μM cholesterol in 50 mM PBS (pH 7.0, 25 °C, −0.7 V).

conducting polymer was not enough to fix the enzyme molecule on the electrode surface. Although the conducting-polymer-based biosensor provides superior biosensor performance, because of their functional architectures, it is not enough to obtain a proper orientation and binding of the enzyme on the electrode. On the other hand, incorporation of the polymeric structures bearing β-CD led to an increase in the biosensor response, as well as serving as an appropriate platform for enzyme deposition. Much attention was given in recent years to the supramolecular complex of β-CD, because of its significance for the selectivity and interactions with the guest molecules and also their industrial importance.[36] Hence, all of these binary interactions were enhanced to hold the biomolecule without losing its biocatalytic activity.

To improve the characteristics of the biosensor, the thickness of the polymeric film was investigated. For this purpose, four bare electrodes coated for different cycles (10, 20, 30, and 40) of electropolymerization were tested to obtain the best amperometric signal by keeping the other parameters constant. If the film layer is not suitable for the stabilization of 3D structure of enzyme molecules, diffusion problems may occur between the PSBTz-coated electrode and the biomolecule. As seen in Figure 8A, the highest response was recorded for the film coated for 20 cycles (64.08 mC, equivalent to a thickness of 99.68 nm).

To examine the effect of pH on the biosensor performance, solutions of pH 6.0, 6.5, 7.0, 7.5 (50 mM PBS, 25 °C), and 8.5 (50 mM sodium bicarbonate buffer, 25 °C) were prepared. In Figure 8B, an optimum response was recorded at pH 7.0. The
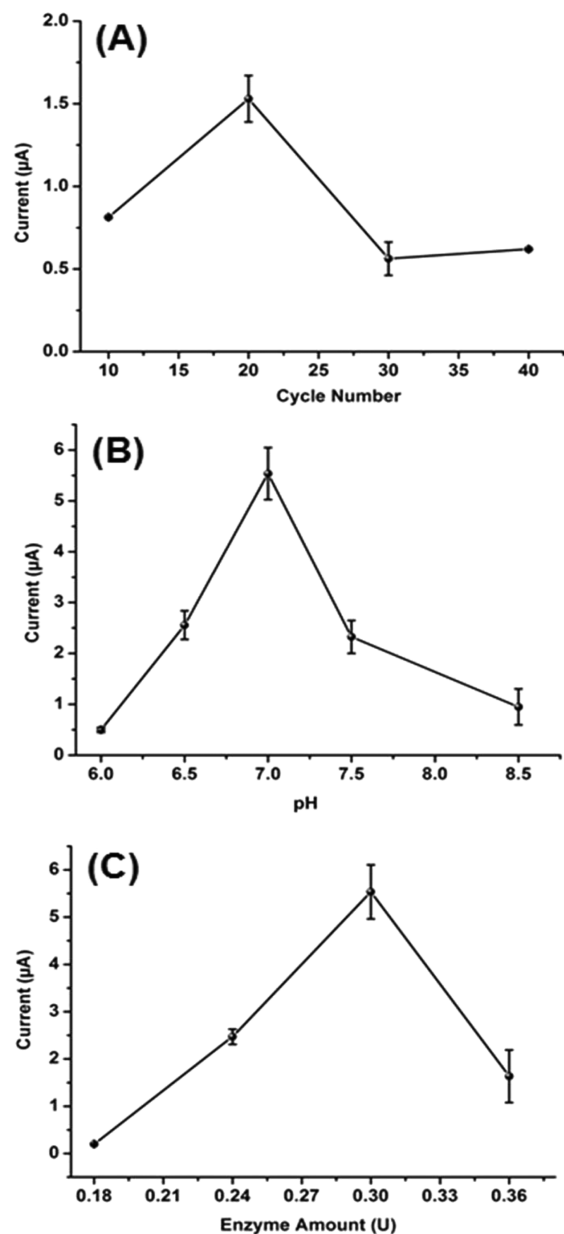
Figure 8. Effect of (A) scan number, (B) pH (50 mM phosphate buffer at pH 6.0, 6.5, 7.0, 7.5, and 50 mM sodium bicarbonate buffer at pH 8.5), and (C) enzyme amount on the biosensor response. Error bars show the standard deviation (SD) of three measurements.

pH of microenvironment can influence the analytical characteristics of enzyme-based biosensors. Extremely high or low pH values may result in the loss of activity bringing low amperometric responses. The optimum amount of enzyme was also investigated and determined as 0.3 U (Figure 8C).

3.4. Electrochemical Characterization of the Electrodes. In order to investigate the changes in the effective surface area after each additional layer on the electrode surface, CV studies were performed in the potential range between 0 and +1.0 V in a solution of 5 mM $Fe(CN)_6^{3-/4-}$ containing 0.1 M KCl and PBS (50 mM, pH 7.0). Successive formation of layers onto the electrode surface resulted in different interfacial structures as seen in Figure 9. Experiments were carried out for
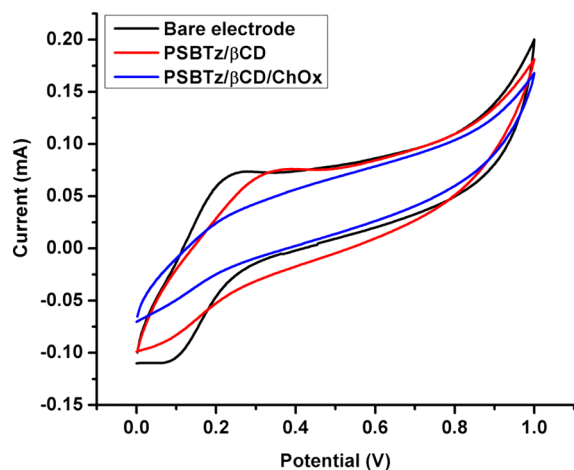

Figure 9. Cyclic voltammograms of graphite bare electrode, as well as PSBTz/β-CD and PSBTz/β-CD/ChOx in 5 mM $Fe(CN)_6^{3-/4-}$ containing 0.1 M KCl and pH 7.0 PBS.

bare graphite electrode as well as PSBTz/β-CD and PSBTz/β-CD/ChOx modified electrodes under optimum conditions. The average value of the electroactive surface area (Ip) was calculated according to the Randles–Sevcik equation:[37]

$$Ip = 2.69 \times 10^5 A D^{1/2} n^{3/2} \gamma^{1/2} C$$

where n is the number of electrons participating in the redox reaction, A is the area of the electrode (cm^2), D is the diffusion coefficient of the molecule in solution ($cm^2\ s^{-1}$), C is the concentration of the probe molecule in the bulk solution (mol cm^{-3}), and γ is the scan rate (V s^{-1}). The increase in the peak currents can be attributed to an increase in the effective surface area. The electroactive surface areas for the bare electrode, PSBTz/β-CD modified electrodes, and PSBTz/β-CD/ChOx modified electrodes were 0.062 cm^2, 0.065 cm^2, and 0.036 cm^2, respectively. As seen in Figure 9, bare electrode exhibited a well-defined oxidation peak (69 μA). After PSBTz/β-CD was coated onto the bare electrode, a slight increase in the oxidation current (73 μA) was observed. This can be attributed to the increase in the effective surface area due to the electrodeposited polymer layer. Moreover, the electrochemically generated supramolecular system (PSBTz/β-CD) may not provide a conductive pathway for electron transfer and promote electron-transfer reactions as much as PSBTz can. Even it is the case, the increase in effective surface area proved that elaboration of polymeric units onto CDs makes the transducer appropriate enough for enzyme immobilization. On such a surface, ChOx was immobilized onto the polymer-coated electrode and the

decrease in the oxidation current (41 μA) was the direct evidence of successful immobilization of enzyme on the modified transducer surface.

3.5. Surface Characterization of the Biosensor. The morphology of the electrode surface was examined by SEM. As shown in Figures 10A–D, the surface morphology was notably changed after each modification. The pristine PSBTz-coated electrode surface can be described as having a typical cauliflower-like structure (Figure 10A). In Figures 10B and 10C, the film depicts a morphology that proves successful coating onto the electrode surface. The porous morphology of the β-CD allowed the homogeneous electropolymerization of the monomer through β-CD surface. Moreover, such a modification proves that the unique structure of the β-CD was protected during the electropolymerization (Figures 10B and 10C). Because of the wrinkled structure of surfaces, enzyme molecules can penetrate into the polymeric layer where enzyme molecules are freely oriented. After the ChOx immobilization, surface was drastically changed and the protein molecules are well-adhered onto this modified surface, because of the high surface area. This homogeneous 3D structure helps stabilization of the enzyme molecules while improving the biosensor performance. Hence, SEM images confirmed successful incorporation of the PSBTz into the β-CD and enzyme deposition on the electrode surface.

3.6. Analytical Characterization. The analytical characterization of the biosensor was investigated with an enzyme electrode constructed under optimum conditions. Biosensor responses were recorded for varying cholesterol concentrations and a calibration curve was obtained (Figure 11). The proposed biosensor showed perfect linearity in a range of 0.15–22.5 μM cholesterol, as given by $y = 0.4093x - 0.0797$ and $R^2 = 0.9908$. Compared to values reported in the literature (0–8 mM for poly(3-TPAA)/ChOx/Pt,[38] 0.05–16.0 μM for KWNTs/ChOx/GCE,[39] 0.01–5.0 mM for GNPs-MWCNTs/ChOx[40]), satisfactory parameters were obtained with the proposed biosensor.

Moreover, the limit of detection (LOD) was also calculated as 0.005 μM, according to $S/N = 3$. This shows the capacity of the biosensor to sense small amounts of substrate. It shows that the LOD is very good, compared to that of other studies. For example, a cholesterol biosensor prepared using a conducting poly(thionine) film gives a LOD value of 6.3 μM.[41] In another example, based on a PEDOT/PMB/ChOx on glassy carbon electrode, the LOD was calculated to be 1.6 μM.[42] In addition, the proposed biosensor showed extremely high sensitivity (5.77 μA/μM cm^2), compared to a cholesterol biosensor (4.49 mA/M cm^2, and ref 41, having a value of 0.18 μA/cm^2/μM).[41]

The biosensor signals corresponding to 25 μM cholesterol were measured six times to prove the repeatability of the biosensor response. The standard deviation (SD) and the relative standard deviation (RSD) were calculated as 0.10 and 4.57%, respectively. Also, operational stability of the biosensor was investigated under optimum conditions. With regard to the stability and durability of the biosensor, there exists only 5% activity loss during 32 measurements upon the addition of a 25 μM substrate. The biosensor showed superior activity over this period while keeping 95% activity of the biomolecule. Kinetic parameters were determined using a Lineweaver–Burk plot.[43] The apparent Michaelis–Menten constant (K_M^{app}) and maximum current (I_{max}) were calculated to be 28.9 μM and 12.1 μA, respectively. A detailed comparison of the properties of the biosensor has been summarized in Table 3.

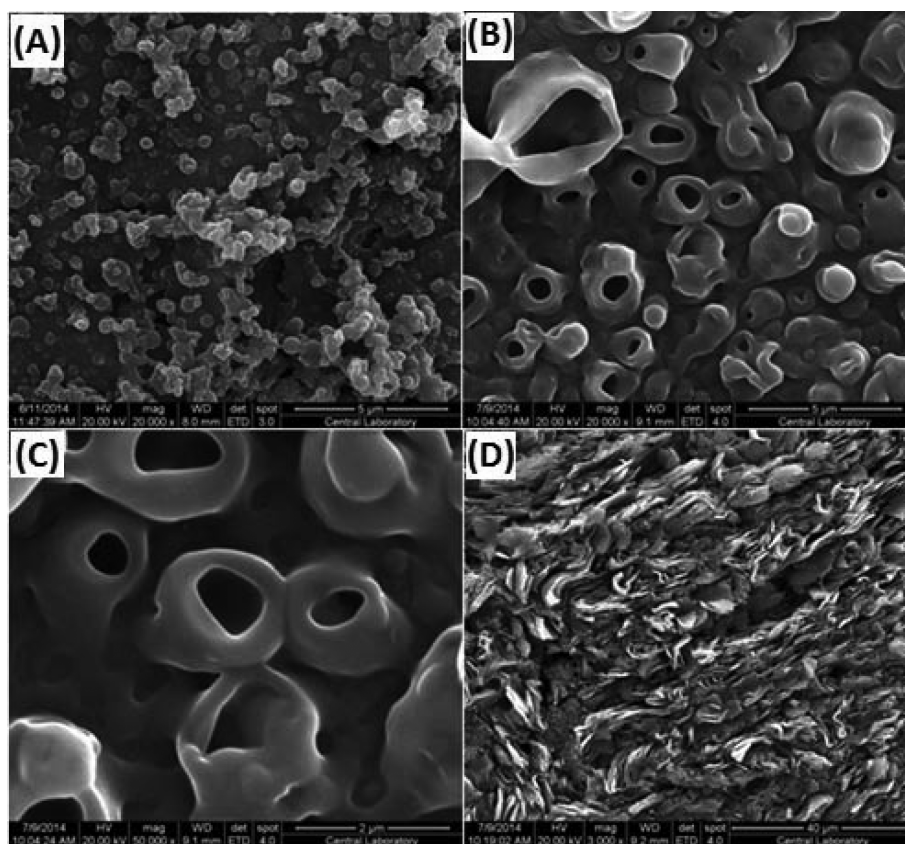**Figure 10.** SEM images showing the surface characteristics of (A) PSBTz, (B) PSBTz/β-CD, (C) PSBTz/β-CD, and (D) ChOx-immobilized PSBTz/β-CD via under optimized conditions.
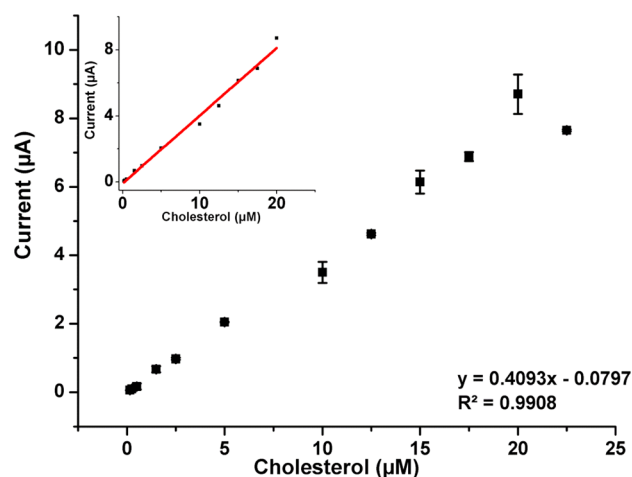

Figure 11. Calibration curve for cholesterol (in 50 mM PBS, pH 7.0, 25 °C, −0.7 V). Error bars show the standard deviation (SD) of three measurements. (Linear range was given as an inset.)

The designed biosensor should be interference-free to obtain a reliable and highly selective response. The effect of potential interferents such as glucose and urea were investigated. For this purpose, these interfering species (in a concentration range of 0.1 mM and 1 mM) were injected to the reaction cell under optimum conditions instead of substrate. The proposed biosensor revealed no response for such interferents. The proposed biosensing system was only selective for cholesterol. Hence, the biosensor can be used for real samples, even in the presence of such interferents during the analysis.

Figure 7B shows the typical current−time (I−t) characteristics of the cholesterol biosensor, measured at various cholesterol concentrations (5 and 10 μM). Figure 7B shows that the proposed biosensor gives an accurate, fast, and reliable response. Thus, successful design of the surface using PSBTz and β-CD shows an appropriate microenvironment for the enzyme molecule while improving the biosensor performance.

3.7. Sample Application. The feasibility of the biosensor for cholesterol detection was tested by analyzing different real

Table 3. Comparison of Some Characteristics of Cholesterol Biosensors Reported in the Literature[a]

immobilization matrix	K_M^{app}/I_{max}	linear range	sensitivity	ref
poly(3,4-ethylenedioxypyrrole)	3.4 mM/34 μA cm^{-2}	NR	10 μA mM^{-1} cm^{-2}	44
poly(3,4-ethylenedioxythiophene)	1.3 mM/17.9 μA cm^{-2}	NR	14.3 μA mM^{-1} cm^{-2}	45
graphene−Pt nanoparticle	5.0 mM/NR	NR	2.07 μA mM^{-1} cm^{-2}	46
ZnO/chitosan	8.63 mg dL^{-1}/NR	5−300 mg dL^{-1}	1.41×10^{-4} A mg dL^{-1}	47
graphene oxide	1.05 mM/NR	0.0005−0.0465 mM	5.71 μA/μM/cm^2	48
PSBTz/β-CD	28.9 μM/12.1 μA	0.15−22.5 μM	5.77 μM/μM cm^2	this work

[a]NR = not reported.

blood serum samples. The serum samples were injected to the cell instead of cholesterol without any pretreatment. The cholesterol contents of the biosensor were estimated from the calibration curve. As shown in Table 4, the results are in good

Table 4. Cholesterol Detection in Serum Samples

sample	hospital data (mM)	PSBTz/ β-CD/ChOx biosensor (mM)	relative error (%)
1	4.57	4.55	0.45
2	5.43	5.33	1.84
3	5.22	5.10	2.22
4	3.88	3.51	9.54

agreement with the values obtained from a local hospital. Therefore, the biosensor is a reliable and accurate tool for cholesterol determination in real samples.

4. CONCLUSIONS

Herein, we have designed and synthesized a novel monomer, SBTz, and developed a novel cholesterol biosensor in combination with β-CD as a new immobilization platform. PSBTz bearing β-CD was prepared by electropolymerization and used as an immobilization platform for ChOx. β-CD served as an excellent biocompatible microenvironment for biomolecule deposition enabling both covalent attachment of the enzyme using its outer hydroxyl groups. PSBTz provided enhanced biosensor performance via retaining activity of the enzyme. The constructed biosensor was characterized in detail by SEM and CV analyses. The biosensor was used to analyze cholesterol content and may act as an alternative sensing system for cholesterol analysis in real samples. The designed biosensor has potential, because of its short response time, easy fabrication, and excellent sensitivity and selectivity.

■ AUTHOR INFORMATION

Corresponding Author
*Tel.: +903122103251. Fax: +903122103200. E-mail: toppare@metu.edu.tr.

Author Contributions
The manuscript was written through contributions of all authors. All authors have given approval to the final version of the manuscript.

Author Contributions
‡These authors contributed equally.

Notes
The authors declare no competing financial interest.

■ ABBREVIATIONS

CPs = conducting polymers
PSBTz = poly(2-(2-octyldodecyl)-4,7-di(selenoph-2-yl)-2H benzo[d][1,2,3]triazole))
β-CD = β-cyclodextrin
ChOx = cholesterol oxidase
CDI = N,N′-carbonyldiimidazole
SEM = scanning electron microscopy
CV = cyclic voltammetry
DCM = dichloromethane
ACN = acetonitrile
TBAPF$_6$ = tetrabutylammonium hexafluorophosphate
NMR = nuclear magnetic resonance
PBS = phosphate buffer solution

SD = standard deviation
RSD = relative standard deviation
K_M^{app} = apparent Michaelis−Menten constant
I_{max} = maximum current

■ REFERENCES

(1) Douhal, A. Ultrafast Guest Dynamics in Cyclodextrin Nano-cavities. *Chem. Rev.* **2004**, *104*, 1955−1976.

(2) Holzinger, M.; Singh, M.; Cosnier, S. Biotin−β-Cyclodextrin: A New Host−Guest System for the Immobilization of Biomolecules. *Langmuir* **2012**, *28*, 12569−12574.

(3) Fulton, D. A.; Stoddart, J. F. Neoglycoconjugates Based on Cyclodextrins and Calixarenes. *Bioconjugate Chem.* **2001**, *12*, 655−672.

(4) Larrañeta, E.; Isasi, J. R. Self-Assembled Supramolecular Gels of Reverse Poloxamers and Cyclodextrins. *Langmuir* **2012**, *28*, 12569−12574.

(5) Nissrin, I.; Dounia, B.; Hanane, Z.; Mohammed, E. K.; Khalid, R. T. The Electrochemical Behavior of Neurotransmitters at a Poly-(Pyrrole-β-Cyclodextrin) Modified Glassy Carbon Electrode. *Anal. Lett.* **2005**, *38*, 1869−1885.

(6) Guo, X.; Abdala, A. A.; Bruce, L.; Lincoln, S. F.; Khan, S. A.; Prud'Homme, R. K. Novel Associative Polymer Networks Based on Cyclodextrin Inclusion Compounds. *Macromolecules* **2005**, *38*, 3037−3040.

(7) Arslan, A.; Kıralp, S.; Toppare, L.; Yagcı, Y. Immobilization of Tyrosinase in Polysiloxane/polypyrrole Copolymer Matrices. *Int. J. Biol. Macromol.* **2005**, *35*, 163.

(8) Işık, S.; Toppare, L.; Cianga, I.; Yağcı, Y. Immobilization of Invertase and Glucose Oxidase in Poly 2-methylbutyl-2-(3-thienyl)-acetate/polypyrrole Matrices. *Eur. Polym. J.* **2003**, *39*, 2375.

(9) Malhotra, B. D.; Chaubey, A.; Singh, S. P. Prospects of Conducting Polymers in Biosensors. *Anal. Chim. Acta* **2006**, *578*, 59−74.

(10) Ramanaviciene, A.; Schuhmann, W.; Ramanavicius, A. AFM Study of Conducting Polymer Polypyrrole Nanoparticles Formed by Redox Enzyme−Glucose Oxidase−Initiated Polymerization. *Colloid Surf. B* **2006**, *48*, 159−166.

(11) Soylemez, S.; Kanik, F. E.; Uzun, S. D.; Hacioglu, S. O.; Toppare, L. Development of an Efficient Immobilization Matrix Based on a Development of an Efficient Immobilization Matrix Based on a Tubes: Synthesis and Its Application to Ethanol Biosensors. *J. Mater. Chem. B* **2014**, *2*, 511−521.

(12) Cosnier, S. Biosensors Based on Electropolymerised Films: New Trends. *Anal. Bioanal. Chem.* **2003**, *377*, 507−520.

(13) Cosnier, S.; Holzinger, M. Electrosynthesized Polymers for Biosensing. *Chem. Soc. Rev.* **2011**, *40*, 2146−2156.

(14) Aurélia, C.; Alain, H.; Pierre, G.; Marguerite, R.; Rachel, A. V. Controlled Synthesis and Inclusion Ability of a Hyaluronic Acid Derivative Bearing α-Cyclodextrin Molecules. *Biomacromolecules* **2006**, *7*, 907−913.

(15) In-Kyu, P.; Horst, A. R.; Shaoyi, J.; Suzie, H. P. Supramolecular Assembly of Cyclodextrin-Based Nanoparticles on Solid Surfaces for Gene Delivery. *Langmuir* **2006**, *22*, 8478−8484.

(16) Kang, M. H.; Tooru, O.; Won, K. L.; Shintaro, S.; Ick, C. K.; Seo, Y. J.; Nobuhiko, Y. Supramolecular-Structured Hydrogels Showing a Reversible Phase Transition by Inclusion Complexation between Poly(ethylene glycol) Grafted Dextran and α-Cyclodextrin. *Macromolecules* **2001**, *34*, 8657−8662.

(17) Julia, J.; Helmut, R. Cyclodextrins in Polymer Synthesis: Free Radical Polymerization of a N-Methacryloyl-11-aminoundecanoic Acid/β-Cyclodextrin Pseudorotaxane in an Aqueous Medium. *Macromolecules* **1999**, *32*, 5236−5239.

(18) Carmen, M.; Gabriela, P. A.; Larissa, G.; María, F. M.; Gustavo, S.; Karen, O. Synthesis of a Thiol-β-cyclodextrin, a Potential Agent for Controlling Enzymatic Browning in Fruits and Vegetables. *J. Agric. Food Chem.* **2013**, *61*, 11603−11609.

(19) Mohsen, A.; Zohre, Z.; Roya, K. Amphiphilic Star Copolymers Containing Cyclodextrin Core and Their Application as Nanocarrier. *Eur. Polym. J.* **2008**, *44*, 1921−1930.

(20) Demirci Uzun, S.; Kayaci, F.; Uyar, T.; Timur, Suna.; Toppare, L. Bioactive Surface Design Based on Functional Composite Electrospun Nanofibers for Biomolecule Immobilization and Biosensor Application. *ACS Appl. Mater. Interfaces* **2014**, *6*, 5235−5243.

(21) Hitoshi, M.; Tatsuya, H.; Yasunori, M. Enzyme Biosensor Based on Plasma-Polymerized Film-Covered Carbon Nanotube Layer Grown Directly on A Flat Substrate. *ACS Appl. Mater. Interfaces* **2011**, *3*, 2445−2450.

(22) Dawei, L.; Lei, L.; Zengyuan, P.; Lei, D.; Qingqing, W.; Huizhen, K.; Fenglin, H.; Qufu, W. Novel Phenolic Biosensor Based on a Magnetic Polydopamine−Laccase Nickel Nanoparticle Loaded Carbon Nanofiber Composite. *ACS Appl. Mater. Interfaces* **2014**, *6*, 5144−5151.

(23) Goff, L.; Holzinger, M.; Cosnier, S. Enzymatic Biosensors Based on SWCNT Conducting Polymer Electrodes. *Analyst* **2011**, *136*, 1279−1287.

(24) Suman, S.; Asha, C.; Malhotra, B. D. Amperometric Cholesterol Biosensor Based on Immobilized Cholesterol Esterase and Cholesterol Oxidase on Conducting Polypyrrole Films. *Anal. Chim. Acta* **2004**, *502*, 229−234.

(25) Sunil, K. A.; Monika, D.; Bansi, D. M. Recent Advances in Cholesterol Biosensor. *Biosens. Bioelectron.* **2008**, *23*, 1083−1100.

(26) Kumar, J.; Souza, S. F. D. Biosensors for Environmental and Clinical Monitoring. *BARC Newsl.* **2012**, *38*, 34−38.

(27) Umar, A.; Rahman, M. M.; Al-Hajry, A.; Hahn, Y. B. Highly-Sensitive Cholesterol Biosensor Based on Well-Crystallized Flower-Shaped ZnO Nanostructures. *Talanta* **2009**, *78*, 284−289.

(28) Chun, X. G.; Zhao, M. S.; Yi, Q. S.; Zhi, L. D.; Chang, M. L. Thin-Walled Graphitic Nanocages As a Unique Platform for Amperometric Glucose Biosensor. *ACS Appl. Mater. Interfaces* **2010**, *2*, 2481−2484.

(29) Dong, W.; Shaojun, Y.; Li, G. L.; Neoh, K. G.; Kang, E. T. Glucose Biosensor from Covalent Immobilization of Chitosan-Coupled Carbon Nanotubes on Polyaniline-Modified Gold Electrode. *ACS Appl. Mater. Interfaces* **2010**, *2*, 3083−3091.

(30) Kim, B.; Yeom, H. R.; Yun, M. H.; Kim, J. Y.; Yang, C. A Selenophene Analogue of PCDTBT: Selective Fine-Tuning of LUMO to Lower of the Band gap for Efficient Polymer Solar Cells. *Macromolecules* **2012**, *45*, 8658−8664.

(31) Cevher, S. C.; Unlu, N. A.; Ozelcaglayan, A. C.; Apaydin, D. H.; Udum, Y. A.; Toppare, L.; Cirpan, A. Fused Structures in the Polymer Backbone to Investigate the Photovoltaic and Electrochromic Properties of Donor-Acceptor Type Conjugated Polymers. *J. Polym. Sci.* **2013**, *51*, 1933−1941.

(32) Henderson, G. T. *Bioconjugate Techniques*, 2nd Edition; Academic Press: Amsterdam, 2008; p 196.

(33) Guo, X.; Abdala, A. A.; May, B. L.; Lincoln, S. F.; Khan, S. A.; Prud'homme, R. K. Novel Associative Polymer Networks Based on Cyclodextrin Inclusion Compounds. *Macromolecules* **2005**, *38*, 3037−3040.

(34) Ravoo, B. J.; Jacquier, J.-C. Host-Guest Interaction between α-Cyclodextrin and Hydrophobically Modified Poly(isobutene-alt-maleic acid) Studied by Affinity Capillary Electrophoresis. *Macromolecules* **2002**, *35*, 6412−6416.

(35) Kumar, T. N.; Ananthi, A.; Mathiyarasu, J.; Joseph, J. K.; Phani, L.; Yegnaraman, V. Enzymeless Creatinine Estimation Using Poly(3,4-Ethylenedioxythiophene)-β-Cyclodextrin. *J. Electroanal. Chem.* **2011**, *661*, 303−308.

(36) Rusa, C. C.; Luca, C.; Tonelli, A. E. Polymer-Cyclodextrin Inclusion Compounds: Toward New Aspects of Their Inclusion Mechanism. *Macromolecules* **2001**, *34*, 1318−1322.

(37) Bard, A. J.; Faulkner, L. R. *Electrochemical Methods: Fundamentals and Applications*, 2nd Edition; John Wiley: New York, 2001.

(38) Nien, P.-C.; Chen, P.-Y.; Ho, K.-C. Fabricating an Amperometric Cholesterol Biosensor by a Covalent Linkage between Poly(3-thiopheneacetic acid) and Cholesterol Oxidase. *Sensors* **2009**, *9*, 1794−1806.

(39) Li, X.-R.; Xu, J.-J.; Chen, H.-Y. Potassium-Doped Carbon Nanotubes Toward the Direct Electrochemistry of Cholesterol Oxidase and Its Application in Highly Sensitive Cholesterol Biosensor. *Electrochim. Acta* **2011**, *56*, 9378−9385.

(40) Zhu, L.; Xu, L.; Tan, L.; Tan, H.; Yang, S.; Yao, S. Direct Electrochemistry of Cholesterol Oxidase Immobilized on Gold Nanoparticles-Decorated Multiwalled Carbon Nanotubes and Cholesterol Sensing. *Talanta* **2013**, *106*, 192−199.

(41) Rahman, M. M.; Li, X.-B.; Kim, J.; Lim, B. O.; Saleh Ahammad, A. J.; Lee, J.-J. A Cholesterol Biosensor Based on a Bi-Enzyme Immobilized on Conducting Poly(Thionine) Film. *Sens. Actuators B* **2014**, *202*, 536−542.

(42) Kakhki, S.; Barsan, M. M.; Shams, E.; Brett, C. M. A. New Redox and Conducting Polymer Modified Electrodes for Cholesterol Biosensing. *Anal. Methods* **2013**, *5*, 1199−1204.

(43) Lineweaver, L.; Burk, D. The Determination of Enzyme Dissociation Constant. *J. Am. Chem. Soc.* **1934**, *56*, 658−666.

(44) Türkaslan, Ö.; Kayahan, S. K.; Toppare, L. A New Amperometric Cholesterol Biosensor Based on Poly(3,4-Ethylenedioxypyrrole). *Sens. Actuators B* **2009**, *136*, 484−488.

(45) Turkarslan, Ö.; Kayahan, S. K.; Toppare, L. Poly(Pyrrole) Versus Poly(3,4- Ethylenedioxythiophene): Amperometric Cholesterol Biosensor Matrices. *J. Solid State Electrochem.* **2009**, *13*, 657−663.

(46) Dey, R. S.; Raj, C. R. Development of an Amperometric Cholesterol Biosensor Based on Graphene-Pt Nanoparticle Hybrid Material. *J. Phys. Chem. C* **2010**, *114*, 21427−21433.

(47) Khan, R.; Kaushik, A.; Solanki, P. R.; Ansari, A. A.; Pandey, M. K.; Malhotra, B. D. Zinc Oxide Nanoparticles-Chitosan Composite Film for Cholesterol Biosensor. *Anal. Chim. Acta* **2008**, *616*, 207−213.

(48) Dey, R. S.; Raj, C. R. Redox-Functionalized Graphene Oxide Architecture for the Development of Amperometric Biosensing Platform. *ACS Appl. Mater. Interfaces* **2013**, *5*, 4791−4798.